J. Dairy Sci. 105:6589–6600
https://doi.org/10.3168/jds.2021-21395

Impact of the electric field intensity and treatment time on whey protein aggregate formation

Robert Axelrod,[1,2] Michael Beyrer,[2]* and Alexander Mathys[1]
[1]ETH Zurich, Laboratory of Sustainable Food Processing, Institute of Food, Nutrition and Health, 8092 Zurich, Switzerland
[2]University of Applied Sciences and Arts Western Switzerland Valais-Wallis (HES-SO VS), Institute of Life Technologies, Food Engineering Group, 1950 Sion, Switzerland

ABSTRACT

Whey proteins are being integrated as high-value food product ingredients due to their versatile and tunable techno-functionality. To meet high food quality and clean label expectations by consumers, electric field (EF) technologies have been proposed to open new frontiers in this field. Despite a variety of studies, it remains ambiguous which EF parameters are crucial to achieving targeted whey protein modifications. Reconstituted liquid whey protein concentrate (WPC_L) and filtered, non-heat-treated liquid whey (WP_{L_filt}) at low protein dry weight concentrations (0.4% wt/wt) were exposed to microsecond pulsed electric field (μsPEF) treatments at EF intensities between 1.25 and 12.5 kV/cm, pulse repetition frequencies between 0.38 and 85 Hz, and pulse lengths set to 10 or 100 μs. Protein aggregations were quantified spectroscopically. We report here that aggregates formed at lower temperatures for μsPEF compared with purely thermal treatments in identical treatment geometries at similar time-temperature profiles. We suggest that the observed increase in absorbance is linked to protein migration, the isoelectric point, local deprotonation phenomena of thiol groups, and cation precipitation. The μsPEF treatment time, which is dependent on the pulse repetition frequency, pulse length, and time of process, is the main driver of the increase in absorbance. High EF intensities balanced with shorter pulse repetition frequencies to ensure similar energy inputs resulted in no aggregate formation. For WP_{L_filt}, 12.5 kV/cm, 10 μs, 0.38 Hz (620 ± 96 kJ/kg; ± standard deviation) did not result in an increase in absorbance, whereas 1.25 kV/cm, 10 μs, 50 Hz (634 ± 57 kJ/kg) with similar time-temperature profiles increased the absorbance at a wavelength of 380 nm by a factor of 8.2 ± 1.7 compared with untreated WP_{L_filt}. In conclusion, the treatment time seems to dominate over high EF intensities at similar energy inputs for aggregate formation and increase in absorbance.

Key words: pulsed electric field, whey protein, aggregation, electrochemistry

INTRODUCTION

Whey proteins have emerged from dairy side-streams as widely used and high-value food product ingredients, allowing a targeted alteration of the viscosity, solubility, foaming, emulsification, and water absorption properties of food matrices (Farrokhi et al., 2019; Inthavong et al., 2019). Edible films and coatings have additionally expanded the appeal of integrating whey proteins into formulations (Ramos et al., 2012; Çakmak et al., 2020). Furthermore, whey proteins are enzymatically hydrolyzed, liberating bioactive peptides and thereby triggering beneficial physiological effects related to the immune system, cardiovascular system, nervous system, and gastrointestinal system (Pihlanto-Leppälä, 2000; Madureira et al., 2010; Dullius et al., 2018). Altering protein structures, whether releasing peptides or generating aggregates, has conventionally resulted in overheating food matrices, thereby lowering the overall food quality, or has culminated in reduced consumer acceptance due to the use of enzymes and increased focus on clean labels. Electric field (**EF**) technologies, such as microsecond pulsed electric field (**μsPEF**) treatments, have been suggested to play a significant role in simultaneously achieving increases in food quality and reducing the necessity of enzymatic treatments (Mikhaylin et al., 2017; Giteru et al., 2018). Various relevant mechanisms for protein modifications have been linked to EF processes, namely ohmic heating, pH shifts, electrochemical reactions, and electrolysis (Meneses et al., 2011; Zhao et al., 2012; Giteru et al., 2018). Modifications and alterations of whey protein structures have been observed in different EF treatment regimes (Giteru et al., 2018). These modifications, briefly summarized, included, for instance, the reduction of the denaturation temperature of β-LG by approximately 4 to 5°C (Perez and Pilosof, 2004), the

Received October 8, 2021.
Accepted March 29, 2022.
*Corresponding author: michael.beyrer@hevs.ch

release of β-LG peptides (Mikhaylin et al., 2017), or the formation of linear fibril-like aggregates in whey protein isolate (Pereira et al., 2016). Studies working with other EF setups, EF regimes, and protein matrices, however, found no protein modification or no additional modification compared with purely thermal treatments with similar time-temperature profiles (Barsotti et al., 2001; Axelrod et al., 2021; Figure 1). Despite the lack of reporting and quantification of crucial treatment parameters (Buchmann et al., 2018; Huppertz et al., 2019), an observed trend is that a less complex treatment setup, such as a batch instead of a continuous system, increased the probability of observing protein structural changes. To achieve a successful industrial implementation of EF technology, allowing the fine-tuning of proteins in the long term, a better understanding of the involved EF mechanisms, of the EF intensity with respect to the treatment time at similar energy inputs, and of the exact location of aggregate formation, is urgently needed.

The aim of this study was thus to observe and quantify aggregations spectroscopically for different EF regimes, to compare the aggregation development against purely thermal treatments with similar time-temperature curves, and to propose mechanisms responsible for aggregate formation. Because heat (cheese making and spray drying) and enzymes (cheese making) result in structural changes of proteins in whey, aggregation trends of reconstituted whey protein concentrate ($\mathbf{WPC_L}$) were compared with a non-heat-treated system containing native whey proteins—that is, filtrated, non-heat-treated whey ($\mathbf{WP_{L\_filt}}$). Gaining more in-depth insights into relevant process windows and involved EF mechanisms could potentially open new chamber design ideas and opportunities to make EF techno-functional tailoring of animal-derived and plant-based proteins industrially feasible in the long term.

MATERIALS AND METHODS

Reconstituted Whey Protein Concentrate

As described elsewhere (Axelrod et al., 2021), spray-dried whey protein concentrate was generously provided and analyzed by Hochdorf Swiss Nutrition AG, Switzerland. Liquid whey concentrate (WPC_L) was reconstituted from the whey protein concentrate powder in ultrapure water (18.2 MΩ·cm, 25°C) at a concentration of 0.5% (wt/wt). The reconstituted liquid (WPC_L) was stirred for 30 min, placed into the refrigerator at 4°C overnight, heated to 55°C for 30 min under constant stirring, and cooled down to room temperature before further usage. The following mean values per 100 g of

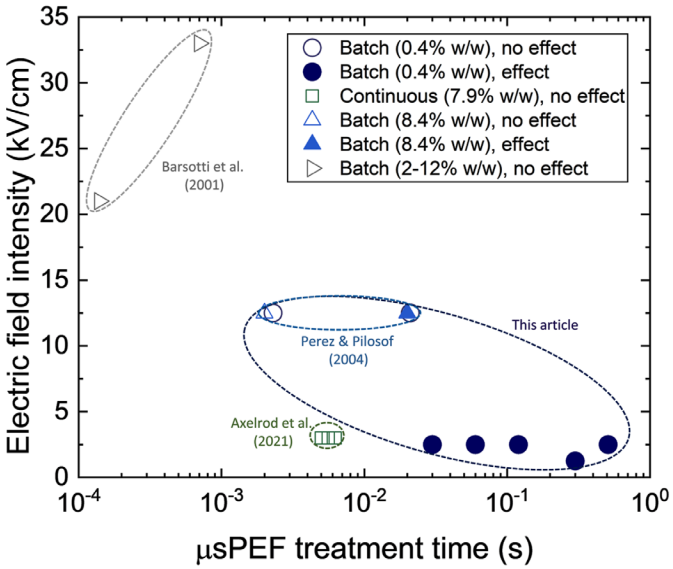

Figure 1. Comparison of the microsecond pulsed electric field (μsPEF) treatment regime, treatment setup, and protein dry weight concentration of whey and whey protein solutions. Empty symbols represent no reported effect or no reported additional effect on whey proteins compared with purely thermal treatments. Filled symbols represent reported effect or reported additional effect on whey proteins compared with purely thermal treatments. Note: Quantification and analysis tools differ between the studies (Barsotti et al., 2001; Perez and Pilosof, 2004; Axelrod et al., 2021).

WPC_L were reported: 24 mg of fat, 395 mg of whey proteins, 68 mg of lactose, 15 mg of ash, 0.86 mg of Na^+, 3.41 mg of K^+, 2.37 mg of Ca^{2+}, 0.30 mg of Mg^{2+}, 1.92 mg of P, and 0.42 mg of Cl^-. The electrical conductivity showed a value of 0.15 mS/cm (SevenCompact conductivity meter, Mettler Toledo) and the pH a value of 6.8 (827 pH Lab, Metrohm AG) at 25°C.

Filtrated, Non-Heat-Treated Whey

Raw centrifugated skim milk (200 L) at a pH of 6.7 at 25°C was kindly provided by Fromagerie d'Étiez (Vollèges, Valais, Switzerland). Non-pasteurized milk serum was obtained by means of cross flow filtration with ceramic membrane modules for microfiltration and ultrafiltration (APV Hemisan). The cutoff was at 0.1 μm, surface area at 0.3 m^2, transmembrane pressure at 0.8 bar, cross flow at 10,000 L/h, and cooling of the recycled feed was performed with tap water at 10°C. To further reduce the conductivity of the serum, allowing for a more stable μsPEF treatment, 90 mL were placed in a dialysis bag (Spectrum Labs Spectra/Por 1 6–8 kDa cellulose, MWCO, Thermo Fisher Scientific), which was sealed and submerged in ultrapure water (18.2 MΩ·cm, 25°C) at 4°C for 24 h. The electrical conductivity and pH in the re-

sulting filtered liquid whey (WP_{L_filt}) were 1.07 mS/cm and 6.8, respectively. The following values were measured per 100 g of WP_{L_filt}: 444 mg of protein, 1.5 g of lactose, 5.28 mg of Na^+, 20.62 mg of K^+, 10.16 mg of Ca^{2+}, 1.99 mg of Mg^{2+}, 7.92 mg of P. The protein concentration was approximated by measuring the total nitrogen content (TOC-L connected to a TN module, Shimadzu Europa) and multiplying the nitrogen content by a factor of 6.25 (Kjeldahl, 1883). Lactose was determined enzymatically (TestKits, R-Biopharm AG) and photometrically. Minerals were quantified by inductively coupled plasma mass spectrometry (iCap ICP-MS, Thermo Fisher Scientific) in helium collision mode. To test the effects of additional free and reactive thiol groups, 0.26, 2.6, and 26 m*M* solutions of L-cysteine hydrochloride (Sigma-Aldrich) were added to WP_{L_filt}. These values were chosen with respect to the approximated free thiol groups in β-LG in the WP_{L_filt} (factors 2, 20, and 200 higher, respectively). To ensure a similar time-temperature profile, the EF intensity was chosen between 0.65 kV/cm and 1.15 kV/cm (Eq. [1]), depending on the added L-cysteine hydrochloride concentrations (0–26 m*M*).

Spectroscopic Measurements

Ultraviolet–visible absorbance measurements (Cary 100, Agilent Technologies Inc.) were conducted for the wavelength range of 320 to 900 nm—that is, examining a potential peak broadening beyond 320 nm due to protein aggregation and quantifying turbidity (Pereira et al., 2016) in the visible light range (380–700 nm). Samples (n = 3) were measured in micro-cuvettes (BrandTech Scientific Inc.) with a sample volume of 70 μL and a light path of 1 cm. Measurements ranging below 300 nm were performed in quartz glass high-performance cuvettes (Hellma GmbH & Co. KG) with a sample volume of 2 mL and a light path of 1 cm (Supplemental Figure S1; https://www.research-collection.ethz.ch/handle/20.500.11850/552192). The instrument was blanked using ultrapure water (18.2 MΩ·cm, 25°C). Samples exceeding an absorbance of 1.5, as was mainly the case for WPC_L, were diluted by a factor of 100 before the measurements.

Pulsed EF and Purely Thermal Treatments

The μsPEF treatments were conducted in electroporation cuvettes (Z706094, Sigma-Aldrich) with a treatment volume (V) of 0.8 mL and a gap size (d) of 0.4 cm. The stainless-steel electrodes were placed in a cuvette holder configuration (Buchmann et al., 2018) and connected to a RUP6-15CL pulse generator (GBS-Elektronik GmbH), which was connected to an external trigger (15 MHz FG300, Yokogawa Electric) that applied unipolar square-wave pulses (Figure 2a; Supplemental Figure S2, https://www.research-collection.ethz.ch/handle/20.500.11850/552192). For WPC_L and WP_{L_filt}, EF intensities (E) were chosen between 1.25 and 12.5 kV/cm, pulse repetition frequencies (f) between 0.38 and 85 Hz, and pulse lengths (τ_p) set to 10 or 100 μs. A voltage probe (P6015A, Tektronix Inc.) and a current monitor (Model 110, Pearson Electronics Inc.) coupled to an oscilloscope (Wave Surfer 10 and Wave Surfer 3000z, Teledyne LeCroy GmbH) were used to fully characterize the pulse shapes at the treatment chamber. All trials were run in triplicate (n = 3).

During a time of process (t) of 5 to 20 min, the specific energy input W_S (kJ/kg) was determined according to Eq. [1] (Raso et al., 2016):

$$W_s = \frac{1}{m}\int_0^{t_{end}} U(t)\cdot I(t)\,dt. \quad [1]$$

Parameter m (kg) represents the mass of the fluid in the treatment chamber, U (V) the voltage amplitude, and I the electric current (A). Although the time of process includes the exposure of the fluid to the electrical pulses and to the heat in between pulses, the μsPEF treatment time includes only pulse exposure time and is given by Eq. [2] (Supplemental Figure S3, https://www.research-collection.ethz.ch/handle/20.500.11850/552192; Raso et al., 2016):

$$t_{PEF} = n\cdot\tau_p. \quad [2]$$

Parameter n corresponds to the number of pulses applied [i.e., time of process multiplied by the pulse repetition frequency (f)]. The pulse length is represented by τ_p (s).

For purely thermal treatments (mainly indirect conductive heat transfer), electroporation cuvettes (V = 0.8 mL, d = 0.4 cm) were placed in the identical cuvette holder configuration and placed in a polystyrene foam climate box ($V \approx 12$ L) equipped with a heating plate and a Pt 100 temperature controller (IKA Werke GmbH & Co. KG; Figure 2b). The air temperature in the climate box was set to be around 65°C. Experiments were run in triplicate (n = 3).

The specific energy Q_s (kJ/kg) introduced by heat, without taking the energy losses from the heat transfer into account, can be approximated by Eq. [3]:

$$dQ_s = c_p(T)\,dT. \quad [3]$$

Parameter T (K) represents the temperature, and c_p [kJ/(kg · K)] signifies the specific heat capacity of the

whey protein solution, which can be approximated by the polynomial shown in Eq. [4] (Kessler, 2002):

$$c_p = (1 - dw) \cdot c_w + 0.135 \cdot dw \cdot c_{carb} + 0.789 \cdot dw \cdot c_{protein} + 0.029 \cdot dw \cdot c_{ash} + 0.047 \cdot dw \cdot c_{fat}. \quad [4]$$

The parameters c_w [kJ/(kg · K)], c_{carb} [1.4 kJ/(kg · K)], $c_{protein}$ [1.6 kJ/(kg · K)], c_{ash} [0.8 kJ/(kg · K)], and c_{fat} [1.7 kJ/(kg · K)] correspond to the specific heat capacity of water, carbohydrates, protein, ash, and fat, respectively. The parameter dw (kg/kg) corresponds to the respective total dry weight concentration.

A fiber optic sensor (TS4, Weidmann Technologies Deutschland GmbH) fully immersed in the fluid logged the temperature at a logging rate of 1 Hz for both μsPEF and purely thermal treatments. Electroporation cuvettes were placed into an ice bath immediately after the treatments and measured spectroscopically within 1 h. Replicates (n = 3) for different parameter combinations were treated by means of randomization. Parameter combinations were chosen to ensure similar time-temperature profiles (i.e., a similar energy input). Electric field intensities were selected with respect to changing the pulse repetition frequency by a factor of maximally 140.

Software and Statistics

Graphing and statistical analyses (mean and SD) were performed in Origin 2019 (OriginLab Corporation). Molecular graphics were created with the UCSF Chimera package (University of California, San Francisco), for which the 1B0O protein data bank file was used (Wu et al., 1999; Pettersen et al., 2004; Tolkach and Kulozik, 2007).

RESULTS AND DISCUSSION

Aggregate Formation

The degree of protein aggregation is crucial for influencing the properties of food matrices (Ryan et al., 2013). Exposing whey to heat during cheese making and spray drying can result in larger aggregates in the initial solution before μsPEF treatment, potentially resulting in an altered aggregation reactivity (Supplemental Figure S4, https://www.research-collection.ethz.ch/handle/20.500.11850/552192; Axelrod et al., 2021). The increased size of protein aggregates after exposure to heat was suggested to be quantifiable by measuring the turbidity (LaClair and Etzel, 2009; Ryan et al., 2012). Indeed, the absorbance of μsPEF untreated WPC_L was larger by a factor of 14.7 ± 2.9 at a wavelength of 380 nm compared with μsPEF untreated WP_{L_filt}.

Treatments of WPC_L with μsPEF (2.5 kV/cm, 10 μs, 85 Hz, 632 ± 15 kJ/kg) resulted in temperatures of 54.4 ± 0.3°C (Figure 3b) and in a protein aggregate layer on the ground electrode (Figure 3d). Taking Eq. [3] and Eq. [4] into account, 126 ± 3 kJ/kg was introduced into WPC_L by heat, without taking the energy losses from the heat transfer into account. Thus, 80 ± 2% of the energy dissipated from the electrodes to

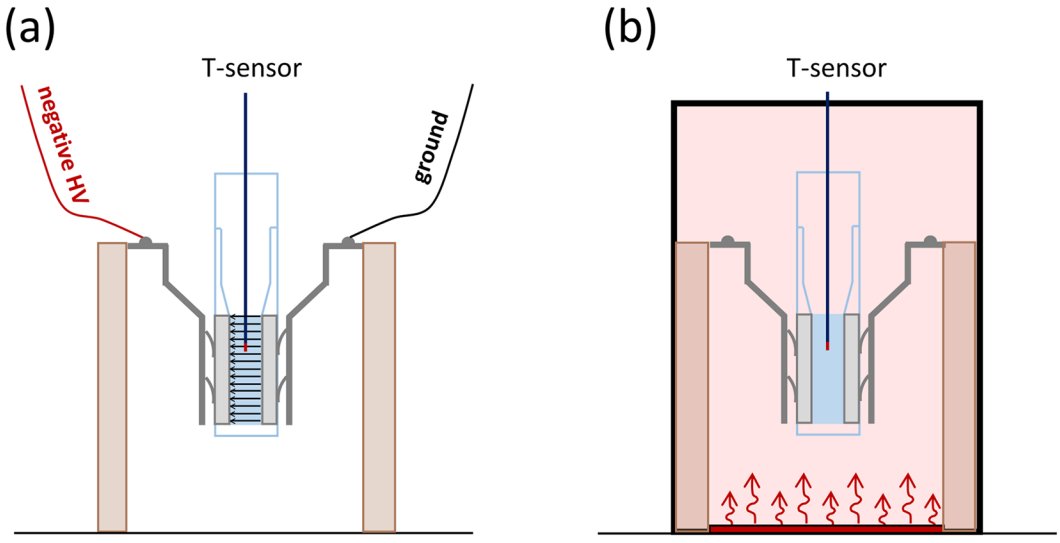

Figure 2. Treatment chamber (volume = 0.8 mL, gap size = 0.4 cm) filled with liquid whey protein concentrate (WPC_L) or filtered, non-heat-treated liquid whey (WP_{L_filt}) placed (a) in an electric field in the range of 1.25–12.5 kV/cm with a pulse repetition frequency of 0.38–85 Hz, and pulse lengths set to 10 μs and 100 μs, or (b) placed into a climate box to achieve similar time-temperature profiles. HV = high voltage.

the surrounding air due to the large surface-to-volume ratio of the batch treatment. Scaling up the volume with respect to the electrode area would have substantial implications on the amount of stored energy. To further validate the whey protein attachment to the electrode, ultraviolet–visible measurements at 380 nm before thoroughly shaking resulted in a decrease of the absorbance by a factor of 2.1 ± 0.1 compared with untreated WPC_L. Vigorous shaking led to an overall increase of the absorbance, and thus to detachment of the protein aggregates from the ground electrode (Figure 3a; Supplemental Figure S5, https://www.research-collection.ethz.ch/handle/20.500.11850/552192).

Aggregate layer formation and absorbance increase due to purely thermal effects in the absence of electrical effects were investigated by placing WPC_L into a climate box in a geometry identical to the μsPEF setup (Figure 2b). Due to the large surface-to-volume ratio of the treatment chamber and the heat flow during μsPEF treatments from the fluid over the electrode to the surrounding air layer, the local temperatures of fluid elements in the near vicinity of the electrodes are lower than or at least equal to fluid elements in the center. Despite the temperature for purely thermal treatments being higher or the same at every time point compared with μsPEF-treated samples (Figure 3b) and tem-

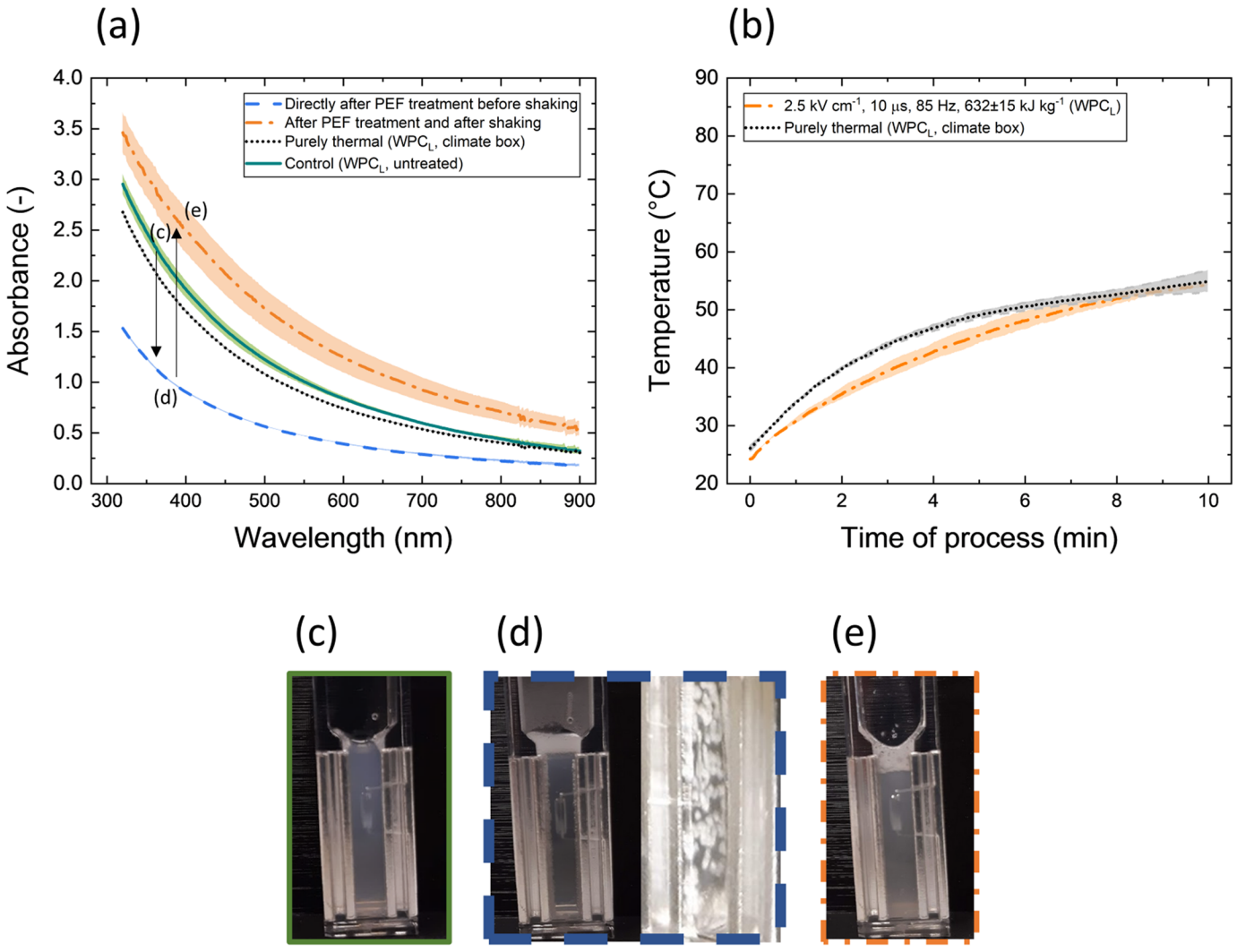

Figure 3. (a) Absorbance spectra of liquid whey protein concentrate (WPC_L; dry weight concentration: 0.5% wt/wt) after heat transfer in the climate box (purely thermal) and after a 10-min pulsed electric field (PEF) treatment (2.5 kV/cm, 10 μs, 85 Hz, 632 ± 15 kJ/kg; ± SD) before and after shaking (n = 3; shaded area represents SD). Shaking refers to the rapid up and down movement of the electroporation cuvettes to detach aggregates from the ground electrode. (b) Time-temperature profile resulting from the ohmic heating effect during microsecond (μs) PEF treatment and after heat transfer in the climate box (purely thermal; n = 3; shaded area represents SD). Visual images of the turbidity in the treatment chamber (c) for untreated WPC_L, (d) after μsPEF treatment but before shaking, with a close-up of the protein aggregate layer on the ground electrode, and (e) after μsPEF treatment and after shaking.

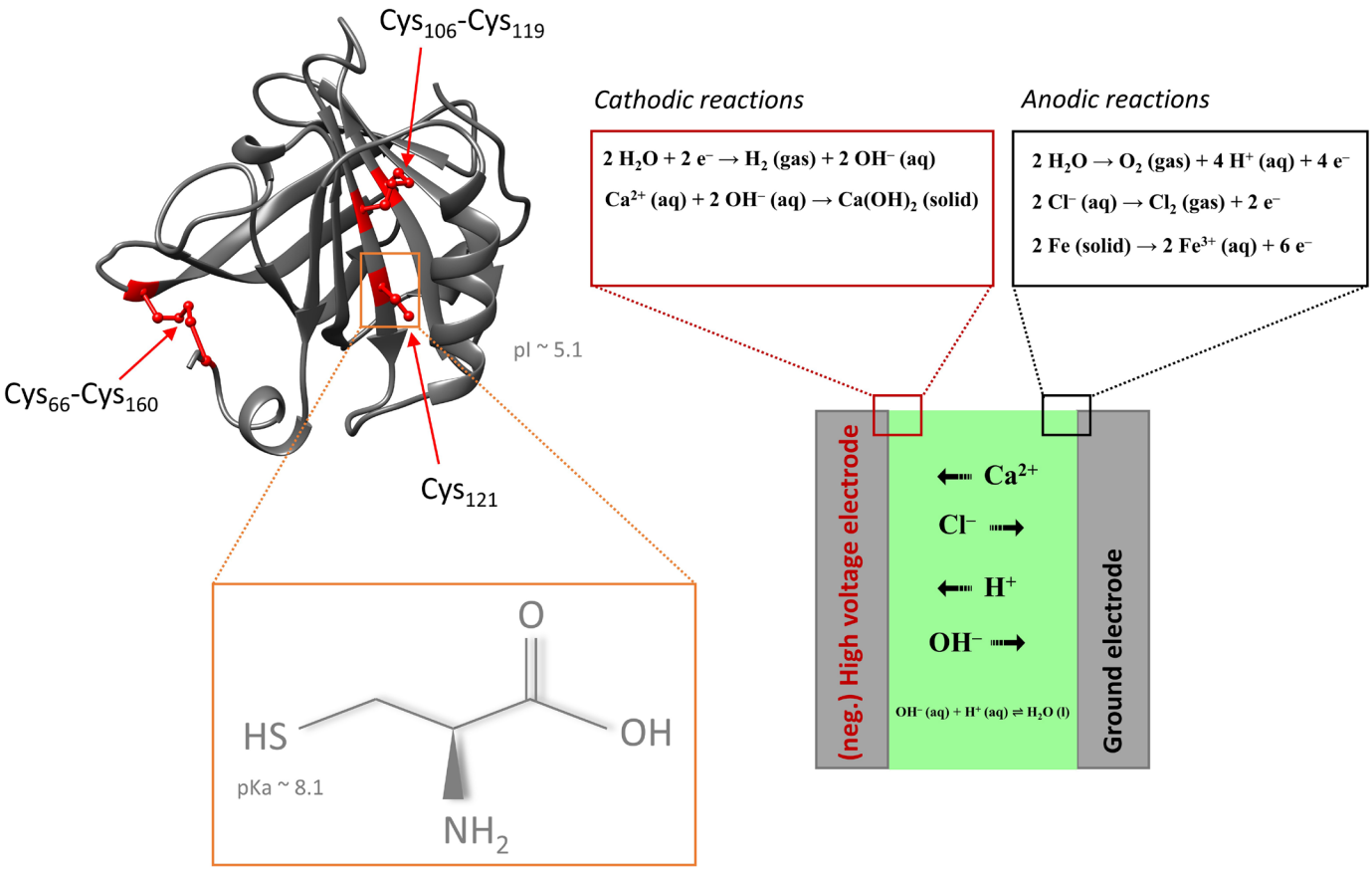

Figure 4. Visualization of the free thiol group embedded in the molecular structure of a β-LG monomer with the chemical structure of an unlinked cysteine AA and relating its pKa to generalized local pH shifts and ongoing chemical reactions during microsecond pulsed electric field treatment based on experiments and simulations done by Saulis et al. (2005) and Meneses et al. (2011). Molecular graphics were inspired and are described by Tolkach and Kulozik (2007). Briefly, the UCSF Chimera package (University of California, San Francisco) and 1B0O protein data bank file were used (Wu et al., 1999; Pettersen et al., 2004). Aq = aqueous.

perature of the electrodes being assumed to be equal or higher compared with the center of the fluid, no aggregate layer and no increase in absorbance was detected (Figure 3a). Moreover, the absorbance even decreased slightly compared with the untreated WPC_L samples, potentially reflecting the fact that the maximal protein reconstitution had not fully been reached.

Considerable protein aggregation resulting from purely thermal treatments occurs at temperatures above 60°C due to the resulting molten globule state of β-LG with exposed reactive thiol groups and hydrophobic regions, if given enough time (Tolkach and Kulozik, 2007). By introducing additional electrical effects, protein aggregate formation can be expected at lower than purely thermal temperatures based on reaching the isoelectric point of β-LG at a value of around 5 (Saulis et al., 2005; Meneses et al., 2011; Engelhardt et al., 2013). Further mechanisms potentially explaining the aggregates below expected purely thermal aggregation temperatures are the deprotonation of thermally exposed (40–55°C) free thiol groups (pKa ≈ 8.1), due to local alkaline conditions, hydroxide formation, and metal ion leakage influencing the structural properties of the proteins (Figure 4; Saulis et al., 2005; Tolkach and Kulozik, 2007; Meneses et al., 2011; Ferreira et al., 2021). The observed aggregate layer during μsPEF treatments at the ground was therefore likely to be related to the electrochemical reactions and the local pH shift impacting cations and the thermally induced accessible reactive thiol group of the β-LG monomer (Figure 4; Supplemental Figure S6, https://www.research-collection.ethz.ch/handle/20.500.11850/552192; Saulis et al., 2005; Tolkach and Kulozik, 2007; Meneses et al., 2011; Ferreira et al., 2021).

To further investigate the potential role of thiol groups in aggregate formation, additional L-cysteine·HCl at concentrations of 0.26, 2.6, and 26 m*M* was added to WP_{L_filt}. These added thiol groups resulted in a gradual

increase of the absorbance after μsPEF treatment, suggesting the importance of the cysteine side chains in terms of the matrix reactivity (Figure 5a). The addition of L-cysteine·HCl did not seem to reduce the increase in absorbance by, for instance, reacting with thiol groups found in β-LG, hindering β-LG interactions. A pure solution of 26 m*M* L-cysteine·HCl also resulted in increased absorbance, further indicating the significance of deprotonated thiol groups. Notably, a pure 5 m*M* $CaCl_2$ solution also resulted in higher absorbance, suggesting that, in addition to thiol reactivity, cation precipitation might play an important role in detecting an increase in absorbance (Figure 5b; Stapulionis, 1999; Saulis et al., 2005; Pataro et al., 2014; Lei et al., 2017). We conclude that the observed increase in absorbance in the whey solutions after μsPEF treatments compared with purely thermal treatments stems from the sufficiently high electrochemical potential (−500 V), most probably resulting in protein migration, increased reactivity of thiol groups, and cation precipitation. Thus, after μsPEF treatment, the absorbance and turbidity increase should in all likelihood be attributed to aggregates resulting from thiol reactivity, hydroxide precipitates, and other chemical species.

Effect of EF Intensity on Protein Aggregation

The EF intensity was increased from 2.5 kV/cm to 12.5 kV/cm, while simultaneously reducing the pulse repetition frequency (***f***) from 85 Hz to 3.5 Hz for WPC_L and from 10 Hz to 0.38 Hz for WP_{L_filt} to ensure a similar energy input (Eq. [1]). Despite choosing a similar energy input, resulting in a comparable time-temperature profile for 12 kV/cm compared with 2.5 kV/cm, no increase in absorbance was detected for 12 kV/cm in both WPC_L and WP_{L_filt} (Figure 6). Purely thermal treatments with similar or higher temperature values at every time point did not result in an increase of the absorbance, and consequently no aggregates were visually observed. Differences between the absorbance of WPC_L and WP_{L_filt}, as previously mentioned, originate from purity differences and heat exposure in pre-processes. Reducing the EF from 2.5 kV/cm to 1.25 kV/cm and increasing *f* from 10 Hz to 50 Hz, once again to ensure similar energy inputs and time-temperature profiles, increased the absorbance for WP_{L_filt}. Although the energy input and the time-temperature profile remained comparable, the treatment time (Eq. [2]) changed drastically, increasing from 21 to 510 ms for WPC_L and from 2.3 to 300 ms for WP_{L_filt} when increasing *f*. It is evident that a longer treatment time, or, in this case, an increased pulse repetition frequency, leads to an increased time for aqueous species to interact and a longer time of deprotonation of the thiol groups, giving the side chains more time to react, interact, and form covalent disulfide bonds, thus increasing the absorbance.

Bringing these observations and hypotheses into the context of 2 highly cited, seemingly contradictory papers in this field results in a plausible explanation. Perez and Pilosof (2004) reported lower denaturation temperatures by using pulsed EF for β-LG compared with purely thermal treatments, whereas Barsotti et al. (2001) reported no significant unfolding of β-LG. Both studies were conducted in batches with plate-plate geometries, applying exponential decay pulses. Two major differences were that Perez and Pilosof (2004) used (1) aluminum-based electrodes, whereas Barsotti et al. (2001) used stainless-steel electrodes. Stainless-steel electrodes produce lower local pH differences than aluminum electrodes (Saulis et al., 2005). Perez and Pilosof (2004) also increased (2) the treatment time by increasing the decaying time of the longest reported pulse from 1.4 μs to 2 ms, while decreasing the maximum number of pulses from 500 to 10. Notably, the EF intensity was around half the value reported by Perez and Pilosof (2004) compared with Barsotti et al. (2001). This further undermines the fact that the treatment time might be more relevant than the EF intensity in terms of changing the protein structure, as Barsotti et al. (2001) reported no significant unfolding of β-LG and Perez and Pilosof (2004) reported a lower denaturation temperature after having applied pulsed EF. The polarity of the pulses was not reported. Both aluminum and stainless-steel electrodes reduce the amount of gaseous chloride at the anode compared with inert electrodes (e.g., platinum) and increase the concentration of metal ions—namely, aluminum and iron, respectively (Saulis et al., 2005; Hedberg and Odnevall Wallinder, 2015). In summary, electrode reactivity and applied treatment times are the most plausible explanations for the different conclusions on whether EF had an additional effect on protein aggregation. In the present study, the increases in absorbance and aggregate formation were detected below purely thermal denaturation temperatures using stainless-steel electrodes, suggesting that the more relevant parameter to be considered here was indeed the μsPEF treatment time.

Effect of Treatment Time on Protein Aggregation

To further investigate the role and significance of the treatment time on protein aggregations, the process times were halved (5 min) and doubled (20 min) with respect to the 10 min seen previously (Figure 7). This changes the exposure of the fluid to the very short elec-

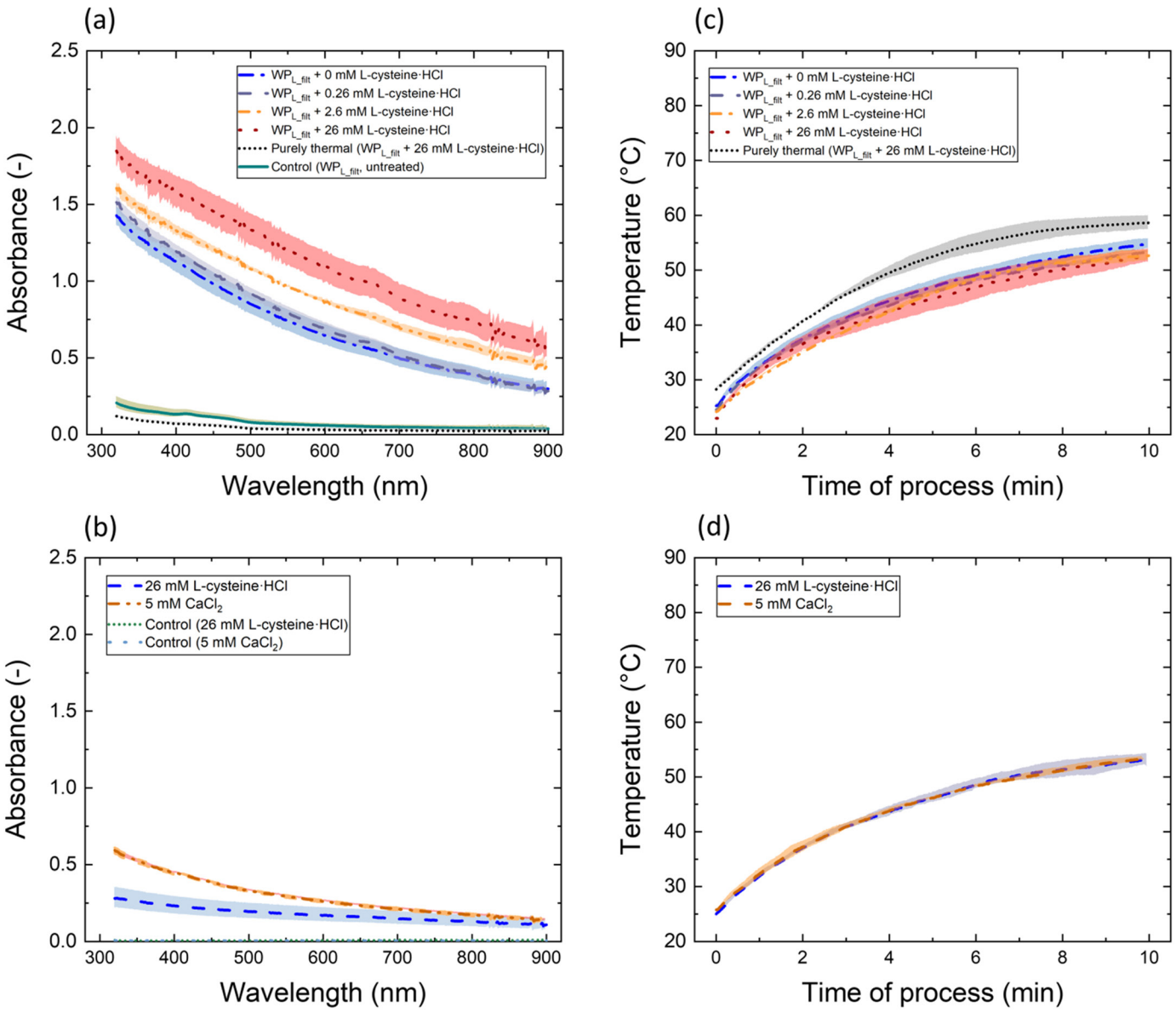

Figure 5. (a) Absorbance for filtered, non-heat-treated liquid whey (WP_{L_filt}) and for (b) pure L-cysteine·HCl and $CaCl_2$ solutions for different AA and ion concentrations after 10 min at a pulse length of 10 µs, a pulse repetition frequency of 50 Hz, and an electric field intensity between 0.65 kV/cm and 1.15 kV/cm, depending on the conductivity to reach a similar time-temperature profile (n = 3; shaded area represents SD). Panels (c) and (d) show corresponding time-temperature profiles resulting from ohmic heating effects during microsecond pulsed electric field treatments or from the heat transfer in the climate box (purely thermal).

trical effects during the pulse peaks (treatment time) as well as the overarching heat exposure originating from the heat capacity of the fluid (time of process). We found that WP_{L_filt} resulted in smaller aggregates than WPC_L, allowing more precise and reproducible results—that is, less precipitation potentially falsifying absorbance measurements related to decrease in absorbance due to protein aggregation. Therefore, WP_{L_filt} was used to further investigate the effect of treatment time on the change in absorbance. Increasing the time of process from 5 to 20 min increased the µsPEF treatment time from 30 to 120 ms and the absorbance at 380 nm from 0.28 ± 0.02 (351 ± 36 kJ/kg, 5 min) to 1.05 ± 0.01 (1,275 ± 153 kJ/kg, 20 min). In terms of energy consumption, time of process, and absorbance increase, reducing the voltage and increasing f seems to be the more industrial relevant approach, as an absorbance at 380 nm of 1.18 ± 0.07 [1.25 kV/cm, 10 µs, 50 Hz, 10 min

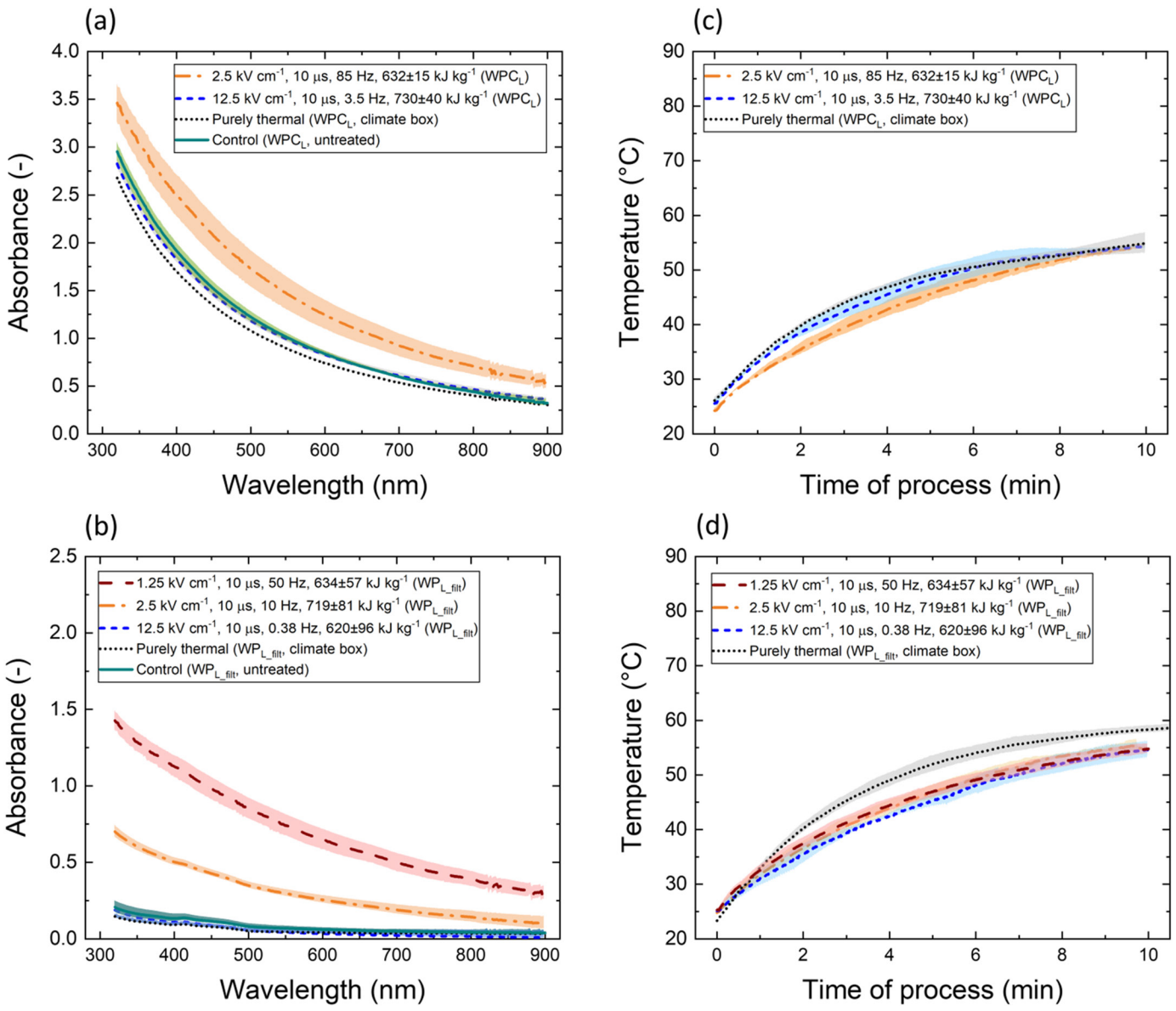

Figure 6. Absorbance spectra for (a) liquid whey protein concentrate (WPC_L) and (b) filtered, non-heat-treated liquid whey (WP_{L_filt}) for different electric field intensities and pulse repetition frequencies quantifying the turbidity partially related to protein aggregations after 10 min (n = 3; shaded area represents SD). Panels (c) and (d) show corresponding time-temperature profiles resulting from ohmic heating effects during microsecond pulsed electric field treatments or from the heat transfer in the climate box (purely thermal).

(634 ± 57 kJ/kg)] was achieved within 10 min (Figure 6). No differences were found when comparing treatments for which the pulse length was increased instead of the pulse repetition frequency; that is, increasing the pulse length from 10 to 100 µs while simultaneously reducing f from 10 Hz to 1 Hz (Figure 8). However, the EF intensity had to be increased by 0.5 kV/cm to ensure an almost identical time-temperature profile. Most likely this originated from the generator control, pulse shape, or differences in heat dissipation. The time of process could potentially be further reduced by further coupling an increased pulse length or pulse repetition frequency with electrode cooling.

When plotting the absorbance of the applied µsPEF parameter combinations as a function of treatment time, it becomes apparent that increases in absorbance and protein aggregation primarily depend on the combination of pulse length and pulse repetition frequency (Figure 9). Energy input and EF intensity seem to play a less significant role in terms of aggregate formation. A similar trend was found for WPC_L (Supplemental Figure S7, https://www.research-collection.ethz.ch/

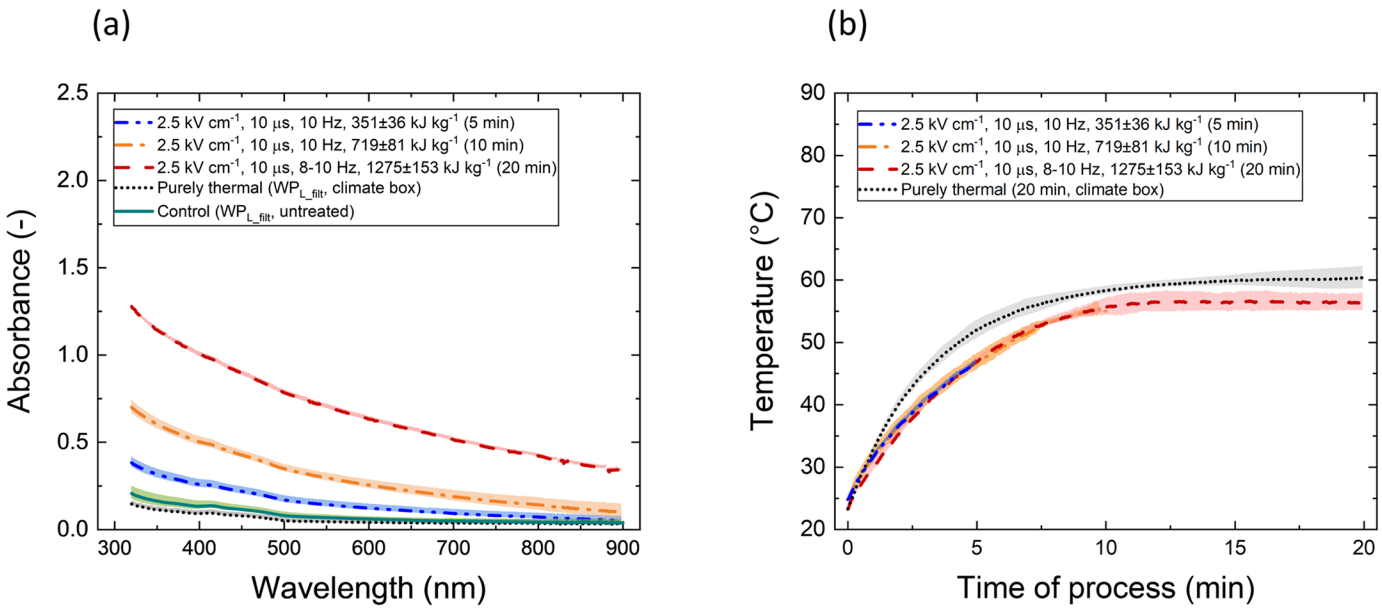

Figure 7. (a) Absorbance spectra for filtered, non-heat-treated liquid whey (WP_{L_filt}) for different times of process (5, 10, or 20 min) quantifying the turbidity development of WP_{L_filt} (n = 3; shaded area represents SD). (b) Corresponding time-temperature profiles resulting from ohmic heating effects during microsecond pulsed electric field treatments or from the heat transfer in the climate box (purely thermal).

handle/20.500.11850/552192). We emphasize that the EF intensity must be large enough to induce formation of reactive species, resulting in a local pH change at the ground, and that the temperature must be high enough (40–55°C) to initiate an intramolecular transition—that is, greater accessibility of the free thiol group (Tolkach and Kulozik, 2007). Finally, the application of pulsed EF, as opposed to direct or alternating current, allows for a more controllable time-temperature profile, while still consistently exposing protein side chains to local pH changes and generating reactivity at the electrodes.

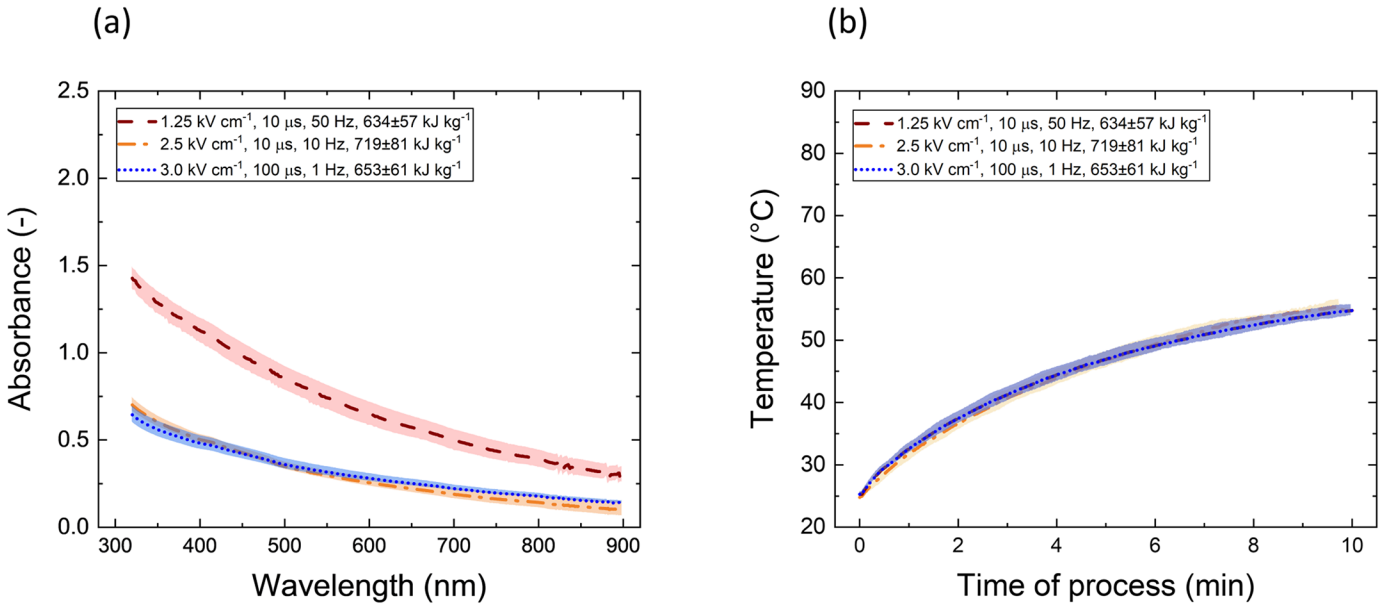

Figure 8. (a) Absorbance spectra for liquid whey protein concentrate for different electric field intensities, pulse repetition frequencies, and pulse lengths quantifying the turbidity related to protein aggregations (n = 3; shaded area represents SD). (b) Corresponding time-temperature profiles resulting from ohmic heating effects during microsecond pulsed electric field treatments.

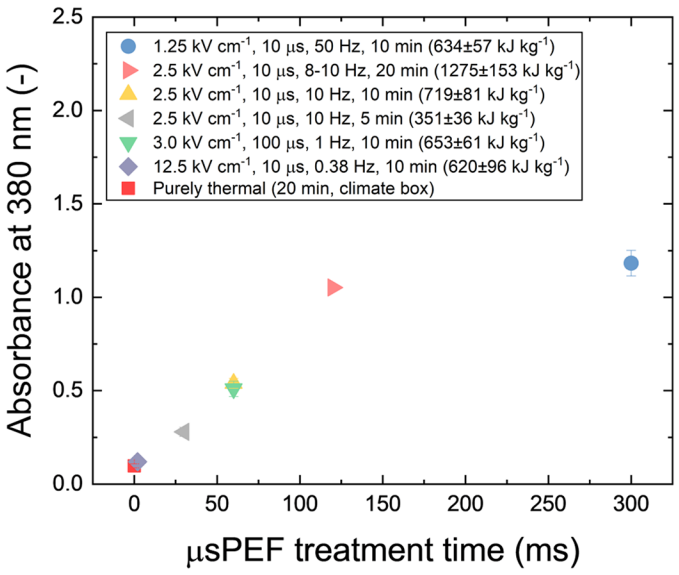

Figure 9. Absorbance at the lower end of the visible wavelength spectrum (380 nm) quantifying the turbidity of filtered, non-heat-treated liquid whey for different microsecond pulsed electric field (µsPEF) treatment times (Eq. [3]) and purely thermal treatments in a climate box with a similar time-temperature profile (n = 3).

CONCLUSIONS

Batch µsPEF treatments of WPC_L and WP_{L_filt} (protein dry weight concentration: 0.4% wt/wt) in a plate-plate geometry (0.8 mL) revealed that the increase in absorbance and the formation of aggregates were highly dependent on µsPEF treatment time—that is, the combination of pulse length and pulse repetition frequency over the time of process (Eq. [2])—and less dependent on EF intensity. Protein migration, the isoelectric point, temporary local deprotonation of thiol groups, and cation precipitation were likely the main drivers for absorbance increase and aggregate formation. Continuous industrial applications of stable aggregate triggering below purely thermal conditions, to control the viscosity of reconstituted products, might be enabled by longer treatment times with adapted geometries.

ACKNOWLEDGMENTS

The authors gratefully thank Christophe Zeder from the ETH Zurich Laboratory of Human Nutrition (Zurich, Switzerland) for inductively coupled plasma mass spectrometry measurements, Lukas Böcker from the Sustainable Food Processing Group at ETH Zurich, Marcel Müller from the Institute for Atmospheric and Climate Science at ETH Zurich, Johannes Burkard from the Laboratory of Food Process Engineering at ETH Zurich, Farida Haidary from the school of Agricultural, Forest and Food Sciences HAFL (Bern, Switzerland), and Adrian Caramaschi from Hochdorf Swiss Nutrition AG (Hochdorf, Switzerland), for their constructive input. Further, the authors thank the ETH Zurich Foundation. This project was financially supported by the Swiss Innovation Agency Innosuisse (Bern, Switzerland; project no. 29439.1 IP-LS). The authors have not stated any conflicts of interest.

REFERENCES

Axelrod, R., J. Baumgartner, E. Tanner, M. Beyrer, and A. Mathys. 2021. Effects of microsecond pulsed electric field (µsPEF) and modular micro reaction system (MMRS) treatments on whey protein aggregation. Int. Dairy J. 123:105170. https://doi.org/10.1016/j.idairyj.2021.105170.

Barsotti, L., E. Dumay, T. H. Mu, M. D. Fernandez-Diaz, and J. C. Cheftel. 2001. Effects of high voltage electric pulses on protein-based food constituents and structures. Trends Food Sci. Technol. 12:136–144. https://doi.org/10.1016/S0924-2244(01)00065-6.

Buchmann, L., L. Böcker, W. Frey, I. Haberkorn, M. Nyffeler, and A. Mathys. 2018. Energy input assessment for nanosecond pulsed electric field processing and its application in a case study with *Chlorella vulgaris*. Innov. Food Sci. Emerg. Technol. 47:445–453. https://doi.org/10.1016/j.ifset.2018.04.013.

Çakmak, H., Y. Özselek, O. Y. Turan, E. Fıratlıgil, and F. Karbancioğlu-Güler. 2020. Whey protein isolate edible films incorporated with essential oils: Antimicrobial activity and barrier properties. Polym. Degrad. Stabil. 179:109285. https://doi.org/10.1016/j.polymdegradstab.2020.109285.

Dullius, A., M. I. Goettert, and C. F. V. de Souza. 2018. Whey protein hydrolysates as a source of bioactive peptides for functional foods—Biotechnological facilitation of industrial scale-up. J. Funct. Foods 42:58–74. https://doi.org/10.1016/j.jff.2017.12.063.

Engelhardt, K., M. Lexis, G. Gochev, C. Konnerth, R. Miller, N. Willenbacher, W. Peukert, and B. Braunschweig. 2013. PH effects on the molecular structure of β-lactoglobulin modified air-water interfaces and its impact on foam rheology. Langmuir 29:11646–11655. https://doi.org/10.1021/la402729g.

Farrokhi, F., F. Badii, M. R. Ehsani, and M. Hashemi. 2019. Functional and thermal properties of nanofibrillated whey protein isolate as functions of denaturation temperature and solution pH. Colloids Surf. A Physicochem. Eng. Asp. 583:124002. https://doi.org/10.1016/j.colsurfa.2019.124002.

Ferreira, S., L. Machado, R. N. Pereira, A. A. Vicente, and R. M. Rodrigues. 2021. Unraveling the nature of ohmic heating effects in structural aspects of whey proteins—The impact of electrical and electrochemical effects. Innov. Food Sci. Emerg. Technol. 74:102831. https://doi.org/10.1016/j.ifset.2021.102831.

Giteru, S. G., I. Oey, and M. A. Ali. 2018. Feasibility of using pulsed electric fields to modify biomacromolecules: A review. Trends Food Sci. Technol. 72:91–113. https://doi.org/10.1016/j.tifs.2017.12.009.

Hedberg, Y. S., and I. Odnevall Wallinder. 2015. Metal release from stainless steel in biological environments: A review. Biointerphases 11:018901. https://doi.org/10.1116/1.4934628.

Huppertz, T., T. Vasiljevic, B. Zisu, and H. Deeth. 2019. Novel Processing Technologies. Elsevier.

Inthavong, W., C. Chassenieux, and T. Nicolai. 2019. Viscosity of mixtures of protein aggregates with different sizes and morphologies. Soft Matter 15:4682–4688. https://doi.org/10.1039/C9SM00298G.

Kessler, H. G. 2002. Food and Bio Process Engineering: Dairy Technology, pages 645–646. Verlag A. Kessler.

Kjeldahl, J. 1883. Neue Methode zur Bestimmung des Stickstoffs in organischen Körpern. Fresenius Z. Anal. Chem. 22:366–382. https://doi.org/10.1007/BF01338151.

LaClair, C. E., and M. R. Etzel. 2009. Turbidity and protein aggregation in whey protein beverages. J. Food Sci. 74:C526–C535. https://doi.org/10.1111/j.1750-3841.2009.01260.x.

Lei, Y., B. Song, R. D. Van Der Weijden, M. Saakes, and C. J. N. Buisman. 2017. Electrochemical induced calcium phosphate precipitation: Importance of local pH. Environ. Sci. Technol. 51:11156–11164. https://doi.org/10.1021/acs.est.7b03909.

Madureira, A. R., T. Tavares, A. M. P. Gomes, M. E. Pintado, and F. X. Malcata. 2010. Invited review: Physiological properties of bioactive peptides obtained from whey proteins. J. Dairy Sci. 93:437–455. https://doi.org/10.3168/jds.2009-2566.

Meneses, N., H. Jaeger, and D. Knorr. 2011. pH-changes during pulsed electric field treatments—Numerical simulation and in situ impact on polyphenoloxidase inactivation. Innov. Food Sci. Emerg. Technol. 12:499–504. https://doi.org/10.1016/j.ifset.2011.07.001.

Mikhaylin, S., N. Boussetta, E. Vorobiev, and L. Bazinet. 2017. High voltage electrical treatments to improve the protein susceptibility to enzymatic hydrolysis. ACS Sustain. Chem.& Eng. 5:11706–11714. https://doi.org/10.1021/acssuschemeng.7b03192.

Pataro, G., G. M. J. Barca, R. N. Pereira, A. A. Vicente, J. A. Teixeira, and G. Ferrari. 2014. Quantification of metal release from stainless steel electrodes during conventional and pulsed ohmic heating. Innov. Food Sci. Emerg. Technol. 21:66–73. https://doi.org/10.1016/j.ifset.2013.11.009.

Pereira, R. N., R. M. Rodrigues, Ó. L. Ramos, F. Xavier Malcata, J. A. Teixeira, and A. A. Vicente. 2016. Production of whey protein-based aggregates under ohmic heating. Food Bioprocess Technol. 9:576–587. https://doi.org/10.1007/s11947-015-1651-4.

Perez, O. E., and A. M. R. Pilosof. 2004. Pulsed electric fields effects on the molecular structure and gelation of β-lactoglobulin concentrate and egg white. Food Res. Int. 37:102–110. https://doi.org/10.1016/j.foodres.2003.09.008.

Pettersen, E. F., T. D. Goddard, C. C. Huang, G. S. Couch, D. M. Greenblatt, E. C. Meng, and T. E. Ferrin. 2004. UCSF Chimera—A visualization system for exploratory research and analysis. J. Comput. Chem. 25:1605–1612. https://doi.org/10.1002/jcc.20084.

Pihlanto-Leppälä, A. 2000. Bioactive peptides derived from bovine whey proteins: Opioid and ace-inhibitory peptides. Trends Food Sci. Technol. 11:347–356. https://doi.org/10.1016/S0924-2244(01)00003-6.

Ramos, O. L., J. C. Fernandes, S. I. Silva, M. E. Pintado, and F. X. Malcata. 2012. Edible films and coatings from whey proteins: A review on formulation, and on mechanical and bioactive properties. Crit. Rev. Food Sci. Nutr. 52:533–552. https://doi.org/10.1080/10408398.2010.500528.

Raso, J., W. Frey, G. Ferrari, G. Pataro, D. Knorr, J. Teissie, and D. Miklavčič. 2016. Recommendations guidelines on the key information to be reported in studies of application of PEF technology in food and biotechnological processes. Innov. Food Sci. Emerg. Technol. 37:312–321. https://doi.org/10.1016/j.ifset.2016.08.003.

Ryan, K. N., B. Vardhanabhuti, D. P. Jaramillo, J. H. van Zanten, J. N. Coupland, and E. A. Foegeding. 2012. Stability and mechanism of whey protein soluble aggregates thermally treated with salts. Food Hydrocoll. 27:411–420. https://doi.org/10.1016/j.foodhyd.2011.11.006.

Ryan, K. N., Q. Zhong, and E. A. Foegeding. 2013. Use of whey protein soluble aggregates for thermal stability—A hypothesis paper. J. Food Sci. 78:R1105–R1115. https://doi.org/10.1111/1750-3841.12207.

Saulis, G., R. Lape, R. Pranevičiute, and D. Mickevičius. 2005. Changes of the solution pH due to exposure by high-voltage electric pulses. Bioelectrochemistry 67:101–108. https://doi.org/10.1016/j.bioelechem.2005.03.001.

Stapulionis, R. 1999. Electric pulse-induced precipitation of biological macromolecules in electroporation. Bioelectrochem. Bioenerg. 48:249–254. https://doi.org/10.1016/S0302-4598(98)00206-2.

Tolkach, A., and U. Kulozik. 2007. Reaction kinetic pathway of reversible and irreversible thermal denaturation of β-lactoglobulin. Lait 87:301–315. https://doi.org/10.1051/lait:2007012.

Wu, S. Y., M. D. Pérez, P. Puyol, and L. Sawyer. 1999. β-Lactoglobulin binds palmitate within its central cavity. J. Biol. Chem. 274:170–174. https://doi.org/10.1074/jbc.274.1.170.

Zhao, W., R. Yang, Q. Liang, W. Zhang, X. Hua, and Y. Tang. 2012. Electrochemical reaction and oxidation of lecithin under pulsed electric fields (PEF) processing. J. Agric. Food Chem. 60:12204–12209. https://doi.org/10.1021/jf304236h.

ORCIDS

Michael Beyrer https://orcid.org/0000-0002-0198-4385
Alexander Mathys https://orcid.org/0000-0003-1633-848X